


 Cite this: *Chem. Commun.*, 2025, 61, 8007

 Received 28th February 2025,
Accepted 23rd April 2025

DOI: 10.1039/d5cc01107h

rsc.li/chemcomm

Multi-cavity discrete coordination cages encapsulating up to four units of pyrazine-*N,N'*-dioxide: molecular soybeans†

 Trilochan Dakua, Srabani Srotoswini Mishra, Ashish Kumar, Shobhana Krishnaswamy  and Dillip Kumar Chand *

A series of Pd₃L₄, Pd₄L₄ and Pd₅L₄-type Multi-Cavity Discrete Coordination Cages (MCDCCs) featuring two, three and four cavities are prepared by complexation of Pd(II) with designer tris-, tetrakis and pentakis-monodentate ligands. The cavities of these MCDCCs encapsulated up to four units of pyrazine-*N,N'*-dioxide (PZDO).

Supramolecular interactions stabilize the overall architectures of biosystems like DNA, proteins, and enzymes to facilitate key processes like molecular recognition and catalysis.^{1,2} To model the multifunctionality and dynamic behaviour of biosystems, a large variety of Single-Cavity Discrete Coordination Cages (SCDCCs) have been prepared *via* metal–ligand self-assembly routes.^{3–8} The Pd(II)-based SCDCCs belong to a special class of molecules having fascinating structural and functional features.^{6–8} The Pd₂L₄ type molecules are the simplest yet most extensively studied among the Pd(II)-based SCDCCs. While the SCDCCs continue to be extensively studied, recent research has shown a new direction towards synthesis and exploration of Pd(II)-based Multi-Cavity Discrete Coordination Cages (MCDCCs).^{6–8} The simplest form of such MCDCCs is represented by the double-cavity Pd₃L₄ type assembly featuring two equal units^{9–15} or unequal units^{16–18} of Pd₂L₄ type 3D cavities that are conjoined at a common metal centre (Fig. 1). The Pd₃L₄ type MCDCCs, capable of binding two guest molecules, are prepared by mixing Pd(II) and a tris-monodentate ligand in 3 : 4 ratio. Subsequently, triple-cavity Pd₄L₄ type MCDCCs having equal¹³ or unequal^{12,17,18} cavities capable of binding three guest molecules (Fig. 1) were prepared by combining Pd(II) and the tetrakis-monodentate ligand in a 4 : 4 ratio. In principle, it should be possible to prepare Pd_{*n*}L₄ type MCDCCs

(*n* ≥ 3) with (*n* – 1) cavities where (*n* – 1) units of Pd₂L₄ type cavities are linearly conjoined. However, only Pd₃L₄ and Pd₄L₄ type MCDCCs are known, whereas Pd₅L₄ type or beyond are not known for the above described Pd_{*n*}L₄ family.

We have recently reported a Pd₂L₄ type SCDCC capable of encapsulating one unit of pyrazine-*N,N'*-dioxide (PZDO) as a guest.¹⁷ In the present work we report a series of Pd₃L₄, Pd₄L₄, and Pd₅L₄ type MCDCCs featuring two, three and four cavities, respectively (Fig. 1). The Pd₂L₄ type sub-frameworks crafted in the new MCDCCs correspond to our reported PZDO-binding Pd₂L₄ type SCDCC. The double-, triple- and quadruple-cavity containing MCDCCs are found to accommodate up to two, three and four units of PZDO, respectively.

The number of seeds in a soybean pod usually ranges from 1 to 4; thus, the family of guest bound SCDCC and MCDCCs is considered here, from a structural viewpoint, as “Molecular Soybeans” in line with “Molecular Peanuts”.¹¹

The bis-monodentate ligand, **L1**, possesses a *meta*-phenylene spacer that is appended with 3-pyridyl groups *via* amide linkages (Fig. 2).¹⁷ Building upon this, we synthesized tris-, tetrakis-, and pentakis-monodentate ligands **L2**, **L3**, and **L4**, respectively (Fig. 2). Detailed procedures for their synthesis

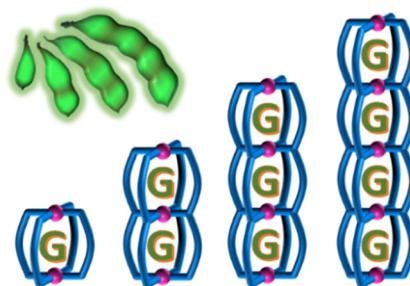


Fig. 1 Cartoon representation of guest-bound Pd₂L₄ type SCDCC and Pd_{*n*}L₄ type MCDCCs featuring (*n* – 1) cavities. Comparison of the architectures with Soybean is shown.

IoE Center of Molecular Architecture, Department of Chemistry, Indian Institute of Technology Madras, Chennai, 600036, India.

E-mail: dillip@zmail.iitm.ac.in

† Electronic supplementary information (ESI) available: Synthesis and characterization of ligands, Pd-complexes, PZDO encapsulation, and crystal structure data. CCDC 2422961. For ESI and crystallographic data in CIF or other electronic format see DOI: <https://doi.org/10.1039/d5cc01107h>

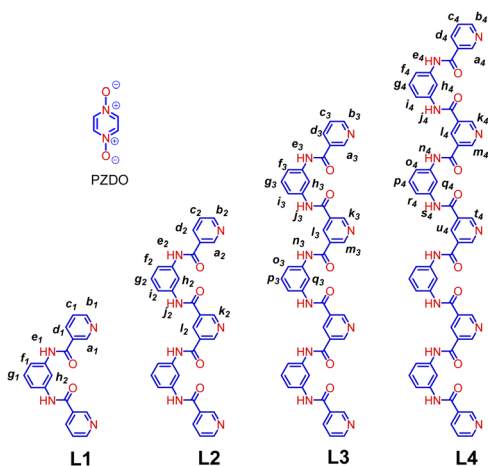


Fig. 2 Chemical structures of the guest PZDO, known ligand **L1**, and new ligands **L2–L4**.

and characterization are provided in the ESI[†] (Schemes S1–S3 and Fig. S1–S27).

Complexation of Pd(NO₃)₂ with **L1**, in a 2 : 4 ratio in DMSO-d₆ predominantly yields a Pd₂L₄ type binuclear assembly, [(NO₃)_x⊂Pd₂(**L1**)₄](NO₃)_{4-x}; **1·4NO₃**, (Fig. 3(i)) along with a minor amount of Pd₃L₆ type cage [(NO₃)_y⊂Pd₃(**L1**)₆](NO₃)_{6-y}; **1'·6NO₃**.¹⁷ We anticipated that complexation of Pd(NO₃)₂ with ligand **L2** in a 3 : 4 molar ratio might result in a Pd₃L₄ type double-cavity cage due to Pd₂L₄ forming behaviour of **L1**. However, the formation of oligomeric products could not be ruled out in advance due to the additional Pd₃L₆ forming nature of **L1**. The complexation reaction was carried out in DMSO-d₆ (ESI,† Scheme S4), which afforded a single discrete product within 20 min, upon stirring at 70 °C, as confirmed from the complexation induced single set of peaks in the ¹H NMR spectrum of the *in situ* prepared or isolated samples (compare Fig. 4(i) with Fig. 4(ii)). We proposed the formation of the double-cavity cage [(NO₃)_{2x}⊂Pd₃(**L2**)₄](NO₃)_{6-2x}; **2·6NO₃** (Fig. 3(ii)) and confirmed the proposal by ESI-MS analysis (ESI,† Fig. S37). The cage was also characterized by various spectroscopic techniques including ¹H, 2D COSY, and 2D NOESY NMR (ESI,† Fig. S28–S30). Formation of a single discrete Pd₃L₄ structure against the probable oligomeric product is attributed to Neighbouring Cage Participation (NCP)¹⁷ where one unit of Pd₂L₄ cavity symbiotically supported the formation of other units that are conjoined with each other.

Complexation reactions of Pd(NO₃)₂, separately with ligand **L3** (4 : 4 molar ratio) and **L4** (5 : 4 molar ratio) were carried out in DMSO-d₆ (ESI,† Scheme S5 and S6). The reaction mixtures were stirred at 70 °C for 12 and 24 hours, respectively, leading to single discrete products as evidenced from single sets of downfield shifted ¹H NMR signals (Fig. 5(ii) and (v)) though slightly broad in nature. The triple cavity system [(NO₃)_{3x}⊂Pd₄(**L3**)₄](NO₃)_{8-3x}; **3·8NO₃** (Fig. 3(iii)) and quadruple cavity system [(NO₃)_{4x}⊂Pd₅(**L4**)₄](NO₃)_{10-4x}; **4·10NO₃** (Fig. 3(iv)) were characterised using ¹H, 2D COSY, and 2D NOESY NMR spectroscopy (ESI,† Fig. S31–S36). The ESI-MS analysis of cages **3·8NO₃** and **4·10NO₃** supported the formation of tetranuclear and pentanuclear systems, respectively (ESI,† Fig. S38 and S39).

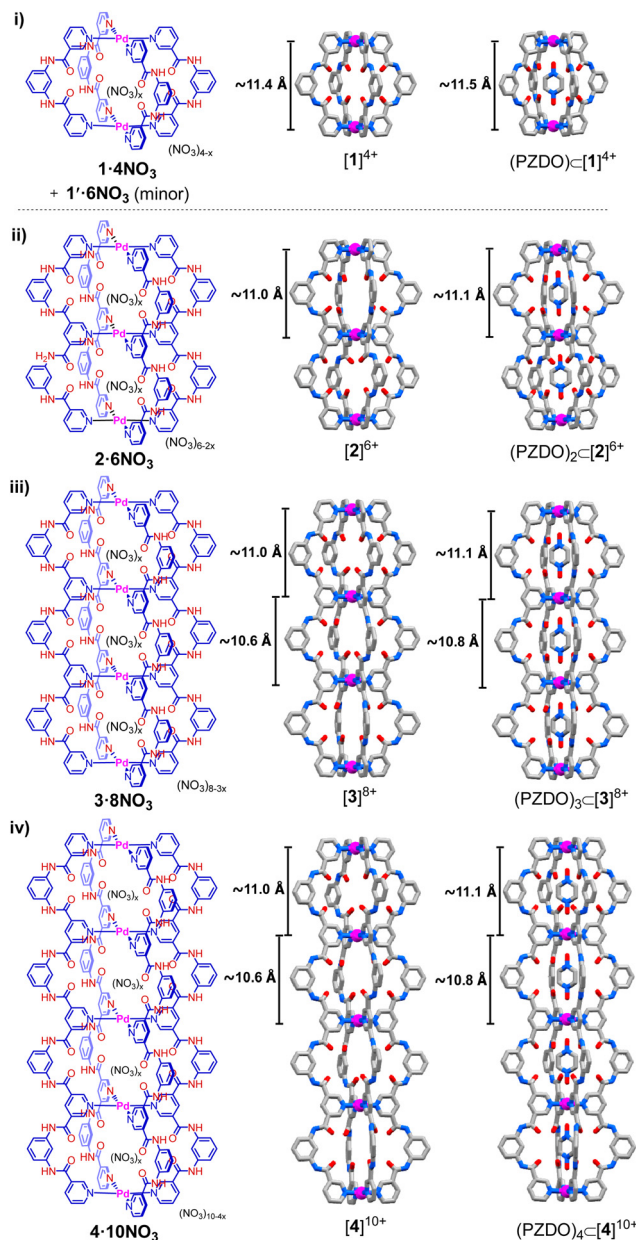


Fig. 3 Chemical structures of the complexes (i) **1·4NO₃**, (ii) **2·6NO₃**, (iii) **3·8NO₃** and (iv) **4·10NO₃** along with gas phase optimized structures (obtained by the DFT method at the [B3LYP/LanL2DZ, 6-31G*] level of theory using Gaussian-16 software) for (i) [Pd₂(**L1**)₄]⁴⁺, [**1**]⁴⁺ and (PZDO)⊂[**1**]⁴⁺; (ii) [Pd₃(**L2**)₄]⁶⁺, [**2**]⁶⁺ and (PZDO)₂⊂[**2**]⁶⁺; (iii) [Pd₄(**L3**)₄]⁸⁺, [**3**]⁸⁺ and (PZDO)₃⊂[**3**]⁸⁺; and (iv) [Pd₅(**L4**)₄]¹⁰⁺, [**4**]¹⁰⁺ and (PZDO)₄⊂[**4**]¹⁰⁺.

Multiple attempts to obtain single crystals of the MCDCCs were unsuccessful. Consequently, we relied on the energy optimized structures to gain insights into their architecture. Notably, the crystal structures of the binuclear complex [Pd₂(**L1**)₄]⁴⁺, [**1**]⁴⁺ revealed the adaptability of the ligand in response to different counter anions.¹⁷ The bound ligand **L1**, in the structure of (PZDO)⊂**1·4NO₃**, adopts a conformation where the C=O groups of **L1** are pointed in an endohedral manner so as to provide optimal host-guest interaction.¹⁷ Energy optimization of [**1**]⁴⁺ was performed by retaining the

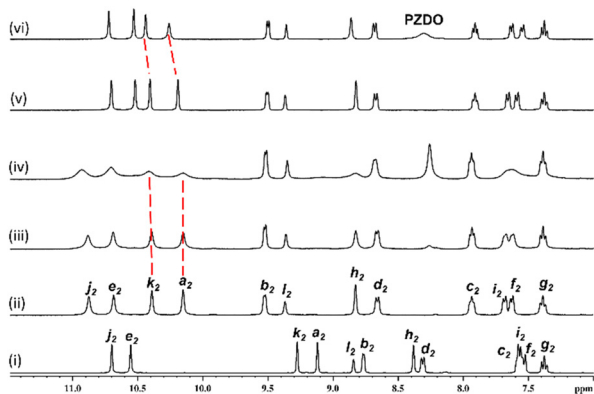


Fig. 4 Partial (400 MHz) ^1H NMR spectra of (i) ligand **L2** recorded at 298 K; (ii) **2-6NO₃** recorded at 298 K; (iii) **2-6NO₃** + 1 equiv. PZDO recorded at 298 K; (iv) **2-6NO₃** + 7 equiv. PZDO recorded at 298 K; (v) **2-6NO₃** recorded at 353 K; and (vi) **2-6NO₃** + 7 equiv. PZDO recorded at 353 K; in DMSO- d_6 , 5 mM conc. with respect to Pd(II).

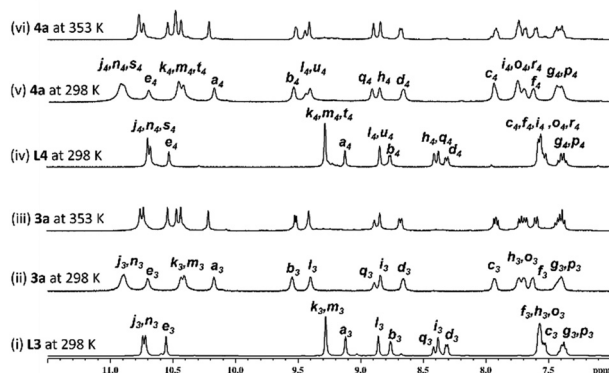


Fig. 5 Partial (400 MHz) ^1H NMR spectra of (i) ligand **L3** recorded at 298 K; (ii) **3-8NO₃** recorded at 298 K; (iii) **3-8NO₃** recorded at 353 K; (iv) ligand **L4** recorded at 298 K; (v) **4-10NO₃** recorded at 298 K; and (vi) **4-10NO₃** recorded at 353 K; in DMSO- d_6 , 5 mM conc. with respect to Pd(II).

same conformation of bound ligand; the Pd–Pd distance in the energy optimised structure was found to be ~ 11.4 Å (Fig. 3(i)).¹⁷ The cationic complexes $[\text{Pd}_3(\text{L}2)_4]^{6+}$, $[\text{2}]^{6+}$; $[\text{Pd}_4(\text{L}3)_4]^{8+}$, $[\text{3}]^{8+}$ and $[\text{Pd}_5(\text{L}4)_4]^{10+}$, $[\text{4}]^{10+}$, were also modelled for energy optimization where all the C=O groups oriented endohedrally (Fig. 3(ii)–(iv)). For cationic complex $[\text{2}]^{6+}$, the observed Pd–Pd distance for both cavities is 11.0 Å, which is slightly smaller than that of $[\text{1}]^{4+}$. In cationic complexes $[\text{3}]^{8+}$ and $[\text{4}]^{10+}$, the peripheral Pd_2L_4 cavities exhibit a Pd–Pd distance of approximately 11.0 Å, while the internal cavities have a Pd–Pd distance of approximately 10.6 Å (ESI,† Fig. S53).

The cages **1-4NO₃**–**4-10NO₃** contain multiple amide bonds, with -NH groups serving as hydrogen bond donors and -C=O groups as acceptors, facilitating guest binding. The cavity of the cage **1-4NO₃** is known to encapsulate one unit of PZDO upon the addition of 4 to 5 equiv. of the guest.

Addition of 1 equiv. of PZDO to a solution of the cage **2-6NO₃** in DMSO- d_6 resulted in a marginal downfield shift of the endohedral α -pyridyl protons, H(a_2) and H(k_2), with peak

broadening indicating host–guest interaction (Fig. 4(iii)). Further addition of PZDO was carried out in a portion-wise manner, approximately 4 equiv. of PZDO per cage molecule (*i.e.* 2 equiv. per cavity), whereupon peak broadening became more pronounced, so much so that peaks due to all endohedral protons (H(a_2), H(k_2) and H(h_2)) and protons *ortho* to amide NH (H(f_2) and H(i_2)) were found to be nearly merged with the base line (ESI,† Scheme S7 and Fig. S44). The ESI-MS analysis of the solution containing the host–guest system revealed the existence of singly occupied, (PZDO) \subset **2-6NO₃** and doubly occupied (PZDO)₂ \subset **2-6NO₃** cages (ESI,† Fig. S51) where the experimentally observed isotopic pattern peaks are found to be comparable with the simulated peaks. Thus, the guest binding experiments presumably resulted in partially as well as completely occupied cavities of the MCDCC; also, there is fast exchange between bound and free guest molecules.

Similarly, portion wise addition of PZDO to the solutions of **3-8NO₃** and **4-10NO₃** and monitoring their ^1H NMR spectra revealed that approximately 6 (*i.e.* 2 equiv. per cavity) and 8 equiv. (*i.e.* 2 equiv. per cavity) of the guest was required, respectively. Further addition of guest to the resulting host–guest mixture showed no significant changes in ^1H NMR of the triple and quadruple cavity systems (ESI,† Fig. S45 and S46). However, the peak broadening in their ^1H NMR spectra is found to be much more pronounced than the case of guest interaction with **2-6NO₃**. Such broadening is attributed to the presence of a large number of amide linkages in the MCDCCs, allowing a higher number of conformational isomers and slow exchange among them. ESI-MS analysis on **3-8NO₃** showed the existence of singly occupied, (PZDO) \subset **3-8NO₃**, doubly occupied (PZDO)₂ \subset **3-8NO₃**, and triply occupied (PZDO)₃ \subset **3-8NO₃** cages (ESI,† Fig. S52). ESI-MS study on the samples prepared using **4-10NO₃** could not provide isotopic pattern peaks matching with corresponding simulated peaks. But we propose the existence of host–guest complexes having partially as well as completely occupied cavities on the basis of NMR study.

To investigate the pronounced peak broadening observed in the ^1H NMR spectra, we examined the host–guest complexation behaviour of the cages **2-6NO₃**–**4-10NO₃** at elevated temperature (353 K) expecting fast conformational changes leading to sharper peaks. Samples were prepared by dissolving the cages **2-6NO₃**–**4-10NO₃** in DMSO- d_6 followed by the addition of 4 to 8 equiv. of PZDO. The ^1H NMR spectra of these samples were recorded at 353 K where the peaks appeared sharper (ESI,† Fig. S47–S49).

For the sample containing **2-6NO₃** and excess (~ 4 equiv.) of PZDO, the ^1H NMR spectrum at 353 K revealed a single set of sharp signals, showing a significant downfield shift of the α -pyridyl protons H(a_2) and H(k_2) indicating guest binding (Fig. 4(v) and (vi)). The ^1H NMR signals corresponding to encapsulated PZDO were not observed in the 10–10.3 ppm region. However, in the region of 8.1–8.4 ppm (free PZDO signal) a broad signal appeared in contrast to the sharp signal of only PZDO recorded at 353 K in DMSO- d_6 , indicating rapid exchange between bound and free PZDO. Similarly, the other cages **3-8NO₃** and **4-10NO₃** showed significant downfield shift of the α -pyridyl protons and binding towards PZDO at high temperature (ESI,† Fig. S50).

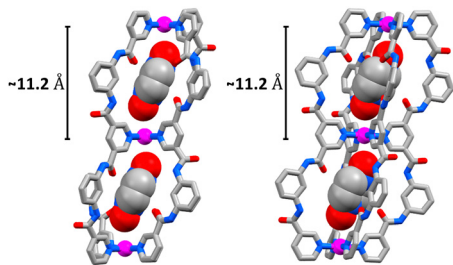


Fig. 6 Crystal structure of $(\text{PZDO})_2 \cdot 2 \cdot 6\text{BF}_4$ in two different orientations. The solvent molecules and counter anions are omitted for clarity.

Although the conjoining units are identical Pd_2L_4 units for $[\mathbf{3}]^{8+}$ and $[\mathbf{4}]^{10+}$, their optimized structures revealed size difference between peripheral and central cavities. The need of energy expensive structural adjustment is probably required to facilitate guest binding, which hinders encapsulation of the guest in all cavities of the MCDCC-type host. To explore this, theoretical modelling of the MCDCCs corresponding to partially as well as completely occupied (by PZDO) cavities was performed. The optimized structures (Fig. 2 and ESI,† Fig. S54–S60) were analysed with respect to the cavity sizes. Optimized structures of fully occupied cages are shown in Fig. 3 and partially occupied cages are collected in the ESI.†

The calculation revealed that guest binding induced the expansion of the cavity size as it occupies the cavity. Interestingly, guest binding induced contraction of the neighbouring cavity that is not occupied by the guest. For example, upon encapsulation of only one guest in one of the cavities of the double cavity system $[\mathbf{2}]^{6+}$, the Pd–Pd distance of the encapsulated cavity increases by ~ 0.3 Å while the adjacent free cavity got contracted by ~ 0.3 Å. Similarly, contraction of adjacent cavities upon PZDO encapsulation was observed for other MCDCCs $[\mathbf{3}]^{8+}$ and $[\mathbf{4}]^{10+}$. On the basis of energy calculation of PZDO (guest), MCDCCs (host), and partially/completely occupied MCDCCs (ESI,† Section S6), “negative cooperativity” for binding of PZDO in the cavities of MCDCCs is proposed. In addition to the slow conformational movement in the ligand backbone, factors like changes in size, existence of cavities that are partially/completely filled by guest molecules and fast exchange between bound and free guest are likely the cause of peak broadening in the NMR spectra.

X-ray diffraction-quality single crystals of $[(\text{PZDO})_2 \cdot \text{Pd}_3(\text{L}2)_4](\text{BF}_4)_6$, $(\text{PZDO})_2 \cdot 2 \cdot 6\text{BF}_4$ were obtained by the slow diffusion of 1, 4-dioxane vapor into a DMSO solution containing PZDO and the cage $2 \cdot 6\text{BF}_4$. The asymmetric unit in the crystals of $(\text{PZDO})_2 \cdot 2 \cdot 6\text{BF}_4$ (monoclinic, $P2_1/c$) contains half a molecule of the trinuclear Pd(II) complex, three BF_4 anions, one dioxane molecule and seven DMSO molecules. The single crystal of $(\text{PZDO})_2 \cdot 2 \cdot 6\text{BF}_4$ displays two molecules of PZDO present inside the cavity (Fig. 6). However, the conformation of ligands in $(\text{PZDO})_2 \cdot 2 \cdot 6\text{BF}_4$ is found to be not identical with that of $(\text{PZDO}) \cdot 1 \cdot 4\text{BF}_4$. One of the PdN_4 planes in $(\text{PZDO})_2 \cdot 2 \cdot 6\text{BF}_4$ is slightly displaced with respect to another by ~ 2.21 Å horizontally and the guest molecules present inside the cage are in a tilted position, resulting in slightly longer $\text{Pd} \cdots \text{O}$ distances. This translates into fewer $\text{C}-\text{H} \cdots \text{O}=\text{C}$

interactions between the guest protons and the carbonyl oxygen of the host. The $\text{C}-\text{H} \cdots \text{O}-\text{N}$ contacts between the α -pyridyl C–H protons of the host and oxygen of PZDO are however, longer and more linear than those in $(\text{PZDO}) \cdot 1 \cdot 4\text{BF}_4$ (ESI,† Table S5).

In summary, we demonstrate the design and synthesis of a set of tris-, tetrakis-, and pentakis-monodentate ligands having strong propensity to form MCDCCs of $[\text{Pd}_3(\text{L}2)_4]^{6+}$, $[\text{Pd}_4(\text{L}3)_4]^{8+}$ and $[\text{Pd}_5(\text{L}4)_4]^{10+}$ types, respectively. During the self-assembly process the ensuing conjoined cavities are found to symbiotically influence each other's construction due to NCP. A novel guest binding behaviour in terms of multi-guest recognition (up to 4 equivalents of PZDO) by the MCDCCs is studied. Thus, our work encourages the construction of multicavity architectures having a large number of linearly conjoined cavities and the exploration of such MCDCCs as a host molecule for novel guest binding behaviours.

D. K. C. thanks Science and Engineering Research Board (SERB), Government of India (project no. CRG/2022/004413) and IIT Madras through a Center under Institute of Eminence program (IoE Phase-II) for financial support. Dedicated to Prof. B. K. Patel on the occasion of his 60th birthday.

Data availability

The data supporting this article have been included as part of the ESI.†

Conflicts of interest

There are no conflicts to declare.

Notes and references

- J. W. Steed and J. L. Atwood, *Supramolecular Chemistry*, John Wiley & Sons, Hoboken, NJ, USA, 3rd edn, 2022, pp. 1–20.
- O. Keskin, A. Gursoy, B. Ma and R. Nussinov, *Chem. Rev.*, 2008, **108**, 1225–1244.
- R. Saha, B. Mondal and P. S. Mukherjee, *Chem. Rev.*, 2022, **122**, 12244–12307.
- E. G. Percástegui, T. K. Ronson and J. R. Nitschke, *Chem. Rev.*, 2020, **120**, 13480–13544.
- T. Y. Kim, R. A. S. Vasdev, D. Preston and J. D. Crowley, *Chem. – Eur. J.*, 2018, **24**, 14878–14890.
- S. Pullen, J. Tessarolo and G. H. Clever, *Chem. Sci.*, 2021, **12**, 7269–7293.
- S. Sharma, M. Sarkar and D. K. Chand, *Chem. Commun.*, 2023, **59**, 535–554.
- A. C. Percy and J. D. Crowley, *Chem. – Eur. J.*, 2023, **29**, e202203752.
- S. Bandi, A. Pal, G. S. Hanan and D. K. Chand, *Chem. – Eur. J.*, 2014, **20**, 13122–13126.
- M. D. Johnstone, E. K. Schwarze, G. H. Clever and F. M. Pfeffer, *Chem. – Eur. J.*, 2015, **21**, 3948–3955.
- K. Yazaki, M. Akita, S. Prusty, D. K. Chand, T. Kikuchi, H. Sato and M. Yoshizawa, *Nat. Commun.*, 2017, **8**, 15914.
- D. Preston, J. E. M. Lewis and J. D. Crowley, *J. Am. Chem. Soc.*, 2017, **139**, 2379–2386.
- R. Zhu, I. Regeni, J. J. Holstein, B. Dittrich, M. Simon, S. Prévost, M. Gradzielski and G. H. Clever, *Angew. Chem., Int. Ed.*, 2018, **57**, 13652–13656.
- J. E. M. Lewis, *Angew. Chem., Int. Ed.*, 2022, **61**, e202212392.
- H. Dasary, M. Sarkar and D. K. Chand, *Chem. Commun.*, 2022, **58**, 8480–8483.
- S. Samantray, S. Krishnaswamy and D. K. Chand, *Nat. Commun.*, 2020, **11**, 880.
- S. S. Mishra, S. Krishnaswamy and D. K. Chand, *J. Am. Chem. Soc.*, 2024, **146**, 4473–4488.
- A. Kumar, S. Krishnaswamy and D. K. Chand, *Angew. Chem., Int. Ed.*, 2025, **64**, e202416332.